Suppression of constant modulus interference in multimode transceivers by closed-loop tuning of a nonlinear circuit

H.Habibi, Y. Wu, J. W. M. Bergmans
Eindhoven University of Technology
Department of Electrical Engineering
Signal Processing Systems
Email: H.Habibi@tue.nl

E. J. G. Janssen, P.G.M. Baltus
Eindhoven University of Technology
Department of Electrical Engineering
Mixed-signal Microelectronics
Email: E.J.G.Janssen@tue.nl

***Abstract*—In multimode transceivers, the transmitter for one communication standard may induce a large interferer in the receiver for another standard. To linearly suppress this interferer, which can be several orders of magnitude larger than the desired received signal, the receiver should have a very large linear dynamic range, resulting in excessive power consumption. Many of potential interferers have a constant modulus modulation. Baier and Friederichs introduced a tuneable nonlinear circuit which can suppress a constant modulus interferer without excessive power consumption. Since an open-loop tuning method is used, the worst-case interference suppression was strongly limited by inaccuracy of circuit components. To alleviate this limitation, we propose a closed-loop tuning method that exploits the locally available interference as side information. Our analysis shows that the proposed method can strongly suppress the interferer while a symbol error rate performance close to that of an exactly linear receiver is achieved. Simulation results for a practical scenario confirm this analysis, and promise much smaller power consumption than for linear interference suppression approaches.**

***Index Terms*—Multimode transceivers, Interference suppression, Nonlinear systems.**

I. Introduction

Nowadays, the mobile phones support services such as data communication, besides voice communication. The phones have become multimode transceivers, supporting several communication standards. From the users' point of view, the simultaneous operation of these transceivers is highly desirable. However, due to the small size of the phones, the local transmitter (TX) of one standard induces a large interference on the local receiver (RX) of another standard. For example, consider simultaneous operation of a WLAN RX operating at 2.4 GHz frequency band and a local GSM TX operating in the 1.8 GHz frequency band. The transmitted GSM signal can be as large as 30 dBm while the WLAN received signal can be as small as -82 dBm [1]. The coupling loss between transceivers in a multimode transceiver is typically between 10 to 30 dB [2]. Hence at the input of the WLAN RX, the power of locally induced interference by the GSM TX can be 102 dB larger than the received desired signal. Hence at the input of the WLAN RX, the locally induced interferer can be 102 dB stronger than the received desired signal.

A typical direct conversion receiver relies on linear filtering to suppress an interferer that has no spectral overlap with the desired signal. Linear filtering can be done by using band-pass filters before and low-pass filters after down-conversion of the received signal. Typically a Surface Acoustic Wave (SAW) filter is used as the band-pass filter and it is placed before the Low Noise Amplifier (LNA) of the receiver to suppress the interferer to some extent. When we consider the WLAN and GSM scenario, the attenuation of state-of-the-art SAW filters is limited to about 40 dB at the GSM frequency band. Hence the GSM interferer can still be 62 dB larger than the WLAN signal after the SAW filter. To prevent nonlinear distortion of the WLAN signal, the receiver Front-End (FE) must linearly amplify and down-convert the combination of the WLAN signal and the interferer before further filtering. Linear processing of the weak WLAN signal in the presence of such large interference requires an excessive linear dynamic range of the receiver FE [3] [4]. Such a dynamic range leads to a high power consumption that is not practical for mobile phones due to their limited energy supply [5].

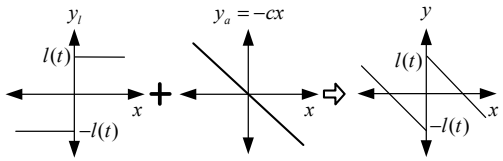

Fig. 1: NIS input-output characteristic.

An alternative approach to linear filtering is to suppress the interference by passing the received signal through special memoryless nonlinearities [6]. An implementation of such a nonlinearity was introduced by Baier and Friederichs [7] to suppress a constant modulus interference. This circuit, which we call Nonlinear Interference Suppressor (NIS), can be built by combining a hard limiter with a tuneable limiting amplitude $l(t)$ and a linear amplifier (with gain of $-c$), as shown in Fig. 1. The hard limiter gain for the small signal is less than the gain for the large signal, because of its compressive behavior.

978-1-4673-0990-5/12/$31.00 ©2012 IEEE

On the other hand the amplifier has the same gain for both small and large signals. Proportional to the envelope of the received interference, $l(t)$ can be tuned such that the gains of the limiter and linear block for the large signal become equal but of opposite sign. Hence the large signal will be strongly suppressed at the NIS output while the desired signal is only attenuated slightly.

The tuning signal in [7] is extracted with an open loop method. In this paper, we will show that the required accuracy of the tuning signal to suppress the interferer below the level of the desired signal can not be achieved by an open loop approach, at least not without cumbersome calibrations. Also such an accuracy can not be easily maintained during the operation due to the environmental changes like temperature. To alleviate this problem, we propose a closed-loop tuning method. We show that with the proposed tuning method we can sufficiently suppress the interference and hence significantly reduce the power consumption of the receiver FE, while achieving a performance close to that of an exactly linear receiver.

II. System model

In this section, we describe the system model of the multimode transceiver that uses the NIS. This model will be used to design a scheme for generation of the tuning signal and to analyze the performance of the RX that uses the NIS.

A. Description of the received signal

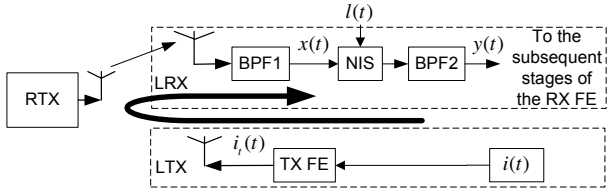

Fig. 2: Multimode transceiver with NIS.

Fig. 2 shows a scenario where a Local TX (LTX) is trying to receive a desired signal, transmitted by a Remote TX (RTX), while the Local TX (LTX) is active. The baseband interferer $i(t)$ with unit power is up-converted by the LTX FE to a center frequency f_i and is transmitted with a power of P_t as: $i_t(t) = \sqrt{2P_t}i(t)\cos(2\pi f_i t + \varphi_i(t))$. At the LRX, the desired signal transmitted by the RTX is received in the presence of a part of $i_t(t)$ coupled from the LTX. The combination of these two signals is passed through a Band Pass Filter (BPF1). The desired signal is passed essentially unchanged through BPF1 and the interferer is attenuated by BPF1. After BPF1, the NIS input $x(t)$ includes both the desired signal and interferer as:

$$x(t)=A_d(t)\cos(2\pi f_d t+\varphi_d(t))+A_i(t)\cos(2\pi f_i t+\varphi_i(t)), \quad (1)$$

where A_d, φ_d, f_d, A_i, φ_i, and f_i are envelope, phase and center frequencies of the desired signal and interferer after the BPF1, respectively. The received signal at the NIS input also includes an additive noise component which is neglected in (1). The main source of the additive noise is the input channel noise. The channel noise at the NIS input is bandlimited by BPF1 and hence its power is much smaller than the desired signal power $P_d = \mathrm{E}(\frac{A_d^2}{2})$, which in turn is much smaller than the interference power $P_i = \mathrm{E}(\frac{A_i^2}{2})$. Later we will see that in the estimation of the tuning signal, the desired signal acts as a disturbing factor. Hence impact of the input noise in (1) on the NIS tuning can be neglected compared to the desired signal. To verify this argument, in simulations in Section IV, we take into account the input channel noise.

In Fig. 2, the TX-RX path of the interference from $i(t)$ to $A_i(t)\cos(2\pi f_i t + \varphi_i(t))$ is shown with a bold line. For practical constant modulus interferers like GSM and Bluetooth the frequency response of BPF1 can be assumed constant over the bandwidth of the interferer. Hence this path can be modeled as a time delay τ and a scaling α and $A_i(t)$ is obtained as:

$$A_i(t) = \alpha\sqrt{2P_t}|i(t-\tau)|. \quad (2)$$

As shown in Fig. 1, the NIS output is the combination of the limiter and amplifier outputs. Using the approximations for the bandpass limiter output [8] for $A_i \gg A_d$, we obtain:

$$\begin{aligned} y(t) \simeq\ & A_{d,y}(t)\cos(2\pi f_d t + \varphi_d(t)) \\ &+\ A_{i,y}(t)\cos(2\pi f_i t + \varphi_i(t)) \\ &+ A_{IM}(t)\cos(2\pi(2f_i - f_d)t + 2\varphi_i(t) - \varphi_d(t)), \end{aligned}$$

where $A_{d,y}$, $A_{i,y}$ and A_{IM} are envelopes of desired signal, interference and main Inter-Modulation (IM) components at the NIS output, respectively and can be approximated by [8]:

$$\begin{aligned} A_{d,y}(t) &\simeq \left(\frac{2l(t)}{\pi A_i(t)} - c\right) A_d(t), \quad (3)\\ A_{i,y}(t) &\simeq \frac{4l(t)}{\pi} - cA_i(t), \\ A_{\mathrm{IM}}(t) &\simeq -\frac{2A_d(t)}{\pi A_i(t)} l(t). \end{aligned}$$

B. Tuning signal

To null the interference, we zero $A_{i,y}(t)$ in (3) and by using (2), we obtain:

$$l_0(t) = \frac{\pi}{4} cA_i(t) = k\sqrt{2P_t}|i(t-\tau)|, \quad (4)$$

where $k = \frac{\pi}{4}c\alpha$. It must be considered that both c and α are slowly varying parameters and their variation rate will not be higher than about 100 Hz. In the multimode transceiver, P_t is known. Hence by estimating k as $\hat{k}$, the tuning signal is generated as:

$$l(t) = \hat{k}\sqrt{2P_t}|i(t-\tau)|, \quad (5)$$

In this paper we only consider constant modulus interferers. In this case $|i(t-\tau)| = 1$ during local transmission and otherwise $|i(t-\tau)| = 0$. The start and stop of the LTX transmission is known. The TX-RX path delay τ is the combination of three parts:

1) Delay of digital blocks of the LTX.
2) The propagation time between LTX and LRX.

3) Group delay of analog filters in TX-RX path.

The first part is constant. Since the path length is about 10 cm, the second part is about 0.3 ns and hence can be neglected. The group delay of the analog filters can be measured beforehand and taken into account. However it may change over time. Generally, the group delay of a bandpass analog filter is about the inverse of its pass-band width. The bandwidth of TX-RX path can not be smaller than the interferer bandwidth. For the WLAN RX and GSM TX scenario, the bandwidth of the GSM TX is 200 kHz. A 1% change in the bandwidth of a 200 kHz filter results in a change of 50 ns in the group delay. Hence by generating $l(t)$ using a pre-measured value of τ we may encounter misalignment of the received interferer with $l(t)$. However the misalignment will not be more than one symbol time of the desired signal and its impact on the receiver performance can be neglected.

C. NIS performance for ideal tuning

Ideally we like to suppress the interference signal and at the same time amplify the desired signal with a time-invariant gain. In this section we analyze the NIS performance in these two respects when the NIS is tuned by the ideal tuning signal $l(t) = l_0(t)$. Based on the simple analysis of (3), for $A_i >> A_d(t)$, the NIS gain for the interferer and the desired signal is 0 and $-\frac{c}{2}$. However a more accurate analysis is required when the difference between A_i and $A_d(t)$ becomes smaller. For $A_i > A_d(t)$, by taking into account a second term in the series expansion for the hard limiter output [9] we obtain:

$$A_{i,y}(t) \simeq \frac{4l_0(t)}{\pi} - cA_i - \frac{l_0(t)}{\pi}\frac{A_d^2(t)}{A_i^2} = -\frac{1}{4}c\frac{A_d^2(t)}{A_i}, \quad (6)$$

$$\begin{aligned} A_{d,y}(t) &\simeq \left(\frac{2l_0(t)}{\pi A_i} - c\right) A_d(t) + \frac{l_0(t)}{4\pi}\frac{A_d^3(t)}{A_i^3} \\ &= -\frac{c}{2}A_d(t) + \frac{c}{16A_i^2}A_d^3(t). \end{aligned} \quad (7)$$

Suppose that Instantaneous Signal to Interference Ratio (SIR) at the NIS input and output are defined as: $\mathrm{ISIR_x} = \left(\frac{A_d(t)}{A_i}\right)^2$ and $\mathrm{ISIR_y} = \left(\frac{A_{d,y}(t)}{A_{i,y}(t)}\right)^2$ respectively. Then using (6) we obtain:

$$\mathrm{ISIR_y} = 4 \ \ \mathrm{ISIR_x}^{-1}. \quad (8)$$

Hence the instantaneous SIR at the NIS output will be 6 dB larger than inverse of the instantaneous SIR at the NIS input.

According to (7), besides the linearly amplified term, a third order component $\frac{c}{16A_i^2}A_d^3(t)$ is also present in $A_{d,y}(t)$. From (7) a 1-dB compression point $A_{1-\mathrm{dB}}$ for the desired signal can be calculated as [3]:

$$A_{1-\mathrm{dB}} = \sqrt{0.145(\frac{c}{2})/(\frac{c}{16A_i^2})} = 1.16A_i. \quad (9)$$

As a rule of thumb, when P_d approaches $\frac{A_{1-\mathrm{dB}}^2}{2}$, the nonlinear distortion becomes evident. Generally a power back-off of about 7 dB from the 1-dB point is required for Orthogonal Frequency Division Multiplexing (OFDM) modulations [10], which results in $10\log_{10}(\frac{P_d}{P_i}) < -6$ dB. In other words, the largest SIR at the NIS input which leads to a negligible distortion for an OFDM signal is about -6 dB. For larger SIRs the interferer is small enough to be handled by the receiver without the NIS aid.

Eq. (8) and (9) can be used to evaluate the NIS performance for scenarios where external interferers are also present. In these scenarios the NIS performance is mainly determined by power ratio of the largest external interferer and the local interferer.

D. Accuracy requirement for $\hat{k}$

Using (5) and (3) we can obtain:

$$A_{i,y}(t) \simeq \frac{4}{\pi}(\hat{k} - k)\sqrt{2P_t}. \quad (10)$$

To prevent wasting the dynamic range of the receiver on the interference, the NIS must suppress the interference such that at the NIS output the interference power $\mathrm{E}(\frac{A_{i,y}^2}{2})$ will be smaller than the desired signal power $\mathrm{E}(\frac{A_{d,y}^2}{2})$, which translates into:

$$\left|\frac{\hat{k} - k}{k}\right| < \frac{1}{2}\sqrt{\frac{P_d}{P_i}}. \quad (11)$$

Hence the magnitude of the estimation error $|\hat{k} - k|$ normalized to k must be smaller than half of the square root of SIR at the NIS input. According to (11), to suppress an interference that can be 60 dB larger than the desired signal at the NIS input, a normalized accuracy of k better than 10^{-3} is required. Consider that $k = \frac{\pi}{4}c\alpha$ is proportional with the power of the received interference and an open loop tuning scheme must measure this power over a wide range of frequencies and input powers. Providing this accuracy with an open loop scheme poses unrealistic constraints on circuit design and fabrication of integrated circuits.

III. Closed-loop tuning of the NIS

In this section we propose a closed-loop tuning method to obtain the tuning signal. We will see that, unlike the open-loop approach, this method does not require such strict conditions on the accuracy of the analog components.

A. Extraction of error signal and feedback loop

To adapt $\hat{k}$ towards k, an error signal should be extracted that indicates $\hat{k} - k$. To this end we need to measure the envelope of the residual interference $A_{i,y}$ at the NIS output. Instead of measuring the power of $y(t)$, we will use the scheme shown in Fig. 3 to measure $A_{i,y}$. We down-convert $y(t)$ using a switching mixer with $x(t)$ as its Local Oscillator (LO) port and $y(t)$ as its Radio Frequency (RF) port. The advantage of this method is that because $x(t)$ is much stronger than $y(t)$ (at least when $\hat{k}$ is close to k), we can use a passive switching mixer with zero power consumption and low complexity. A switching mixer changes the sign of its RF input based on the sign of its LO input as:

$$\eta(t) = y(t)\mathrm{sign}(x(t)), \quad (12)$$

where $\text{sign}(x(t)) = \{1, x(t) > 0; 0, x(t) = 0; -1, x(t) < 0\}$. In appendix I, we prove that for $A_d << A_i$:

$$\eta(t) \simeq \frac{8}{\pi^2}\sqrt{2P_t}\left(1 + \frac{1}{2}\frac{A_d^2(t)}{\alpha^2 2P_t}\right)(\hat{k} - k) + \nu(t), \qquad (13)$$

where

$$\nu(t) = \frac{8}{\pi^2}\left(\frac{\hat{k}}{2} - k\right)\frac{A_d}{\alpha}\cos(2\pi(f_d - f_i)t + \varphi_d(t) - \varphi_i(t))$$

acts as a disturbance term in the estimation of k. The disturbance term $\nu(t)$ is centered at $f_d - f_i$ and its bandwidth is the sum of bandwidths of the desired signal and interferer. The feedback loop is required to track the changes of k which are in the order of 100 Hz. In a practical scenario, the frequency separation $f_d - f_i$ between the desired signal and interferer is so large that $\nu(t)$ has no spectral content in the passband of the feedback loop. Hence $\nu(t)$ will have a zero mean and have no impact on the steady state solution of the loop. According to (13), by neglecting the disturbance term, when $\hat{k} > k$: $\eta(t) > 0$ and when $\hat{k} < k$: $\eta(t) < 0$. Hence by integrating $-\eta(t)$ we can steer $\hat{k}$ towards k. The complete feedback loop is shown in Fig. 3, where $\eta(t)$ is multiplied by a scaling factor $-\mu$ and integrated. The feedback loop forces the average of the integrator input towards zero which results in $\hat{k} = k$ in the steady state.

Here the only source of the analog circuit's impairment that can affect the steady state of the loop is the presence of a DC bias at the mixer output. The inaccuracies in input-output characteristics of the switching mixer results in slight changes of the loop gain which is not crucial. The proposed topology benefits from a passive mixer which can be implemented with a small DC bias.

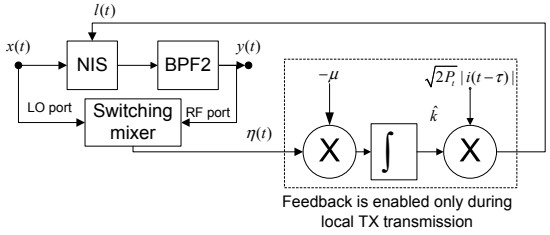

Fig. 3: Feedback loop for adaptation of $\hat{k}$.

B. Dynamic behavior of the loop

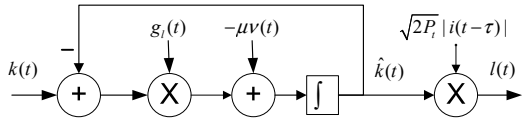

Fig. 4: Behaviorial model of the feedback loop.

Fig. 4 shows a behaviorial model of the first-order feedback loop in Fig. 3 based on (13). The loop's dynamics is determined by the total gain $g_l(t)$ from output of the integrator to its input as:$g_l(t) = \frac{8}{\pi^2}\sqrt{2P_t}(1 + \frac{A_d^2(t)}{4\alpha^2 P_t})\mu$. Because the NIS is used for scenarios where P_d is much smaller than $P_i = \alpha^2\sqrt{2P_t}$, to study the dynamic behavior of the loop we can approximate the total gain as: $g_l \simeq \frac{8}{\pi^2}\sqrt{2P_t}\mu$. The loop time constant equals the inverse of g_l. A fixed total gain is required to have a fixed convergence time of the loop. To make g_l independent of P_t, we can use a variable scaling factor as: $\mu = \frac{\pi^2\mu_0}{8\sqrt{2P_t}}$, where μ_0 is a constant equal to the 3-dB bandwidth of the loop, (in radian/s). Since P_t is known in the multimode transceiver, such a variable scaling factor can be implemented easily.

The group delay of the first-order loop is about $\frac{1}{\mu_0}$ in its pass-band. Hence for a time varying $k(t)$, there will be a delay from $k(t)$ to $\hat{k}(t)$. Since α changes much faster than c, to study the dynamic response of the loop we consider only variations of α. As a special case we consider sinusoidal variations of $\alpha(t)$ around a fixed value as:

$$\alpha(t) = \alpha_0 + \alpha_1\cos(\omega_\alpha t). \qquad (14)$$

The error originating from the time lag is obtained as:

$$\left|\frac{\hat{k}(t) - k(t)}{k(t)}\right| = 2\frac{\alpha_1}{\alpha(t)}\left|\sin(\frac{\omega_\alpha}{2\mu_0})\sin\left(2\omega_\alpha t + \frac{\omega_\alpha}{\mu_0}\right)\right|. \qquad (15)$$

To suppress the interference to a level below that of the desired signal (11) must be satisfied. For small values of $\frac{\omega_\alpha}{2\mu_0}$, this is true when we choose μ_0 such that:

$$\mu_0 > 2\omega_\alpha\alpha_1\sqrt{\frac{P_t}{P_d}}. \qquad (16)$$

According to (16) the required value for μ_0 is determined by:

1) the frequency of changes of $\alpha(t)$,
2) the amplitude of these changes α_1,
3) the worst-case ratio of the transmitted signal power P_t to the received desired signal power P_d.

In the next section we see that typical values of these parameters lead to a reasonable constraint on μ_0.

IV. Simulation results

In this section, the simulation results for the WLAN RX and GSM TX scenario are presented. The simulation parameters are listed in Table. I. The OFDM modulation has 64 sub-carriers and each subcarrier uses 16-QAM modulation. We assume that the received WLAN signal is passed through an Additive White Gaussian Noise (AWGN) channel. For a linear receiver, the SER performance depends only on the desired Signal to Noise Ratio (SNR), where the noise power

TABLE I: Simulation parameters.

	LRX	LTX
Standard	WLAN	GSM
Frequency	2.4 GHz	1.8 GHz
Bandwidth	20 MHz	0.2 MHz
Modulation	OFDM	GMSK
Power (50 Ω system)	P_d:minimum 10^{-11} W (-80 dBm)	P_t: Maximum 1 W (30 dBm)

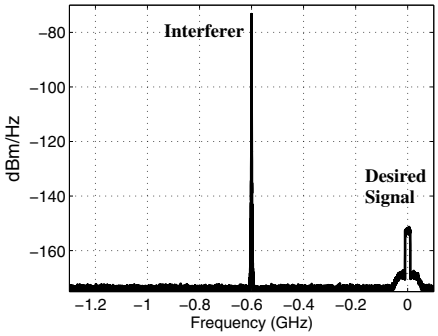

(a) PSD at NIS Input.

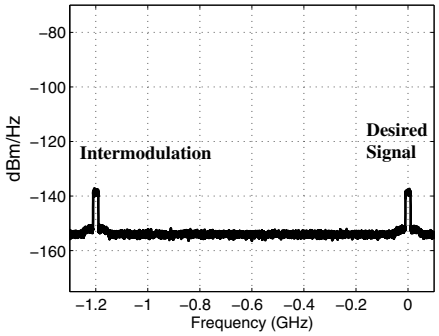

(b) PSD at NIS output, constant α.

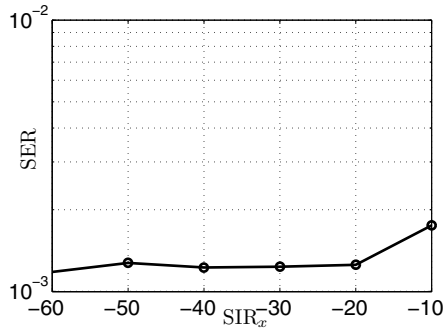

(c) SER vs. SIR$_x$, constant α.

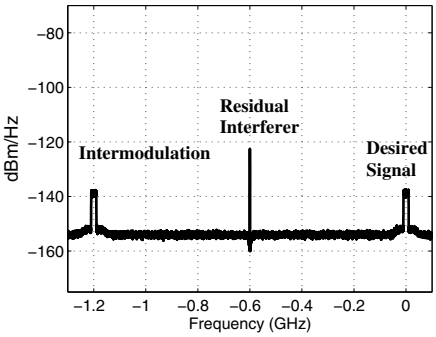

(d) PSD at NIS output, time varying $\alpha(t)$.

Fig. 5: Simulation results.

is measured in the frequency channel of the desired signal. We have chosen an SNR of 17.6 dB which results in an un-coded SER of 10^{-3} for an exactly linear receiver [11], leading to a negligible SER after forward error correction in the WLAN receiver. The TX-RX coupling can be between -10 dB and -30 dB and the GSM signal is further attenuated 40 dB by BPF1. For the steady state simulations we use a constant value of $10^{-2.5}$ for α, which is the combination of worst case coupling of -10 dB and BPF1 attenuation of 40 dB. For simulations of dynamic behavior, we assume that the TX-RX coupling changes sinusoidally so that:

$$\alpha(t) = (0.55 + 0.45\cos(2\pi 100t)) \times 10^{-2.5}, \qquad (17)$$

which reflects a 20 dB change of α from -50 dB to -70 dB. In all cases we have chosen $\mu_0 = 5.6 \times 10^5$ radian/s which is equivalent to a 89 kHz 3-dB bandwidth of the feedback loop. According to (16), this value of μ_0 results in suppression of the interference to a level below that of the desired WLAN signal with a power of -80 dBm for a time varying $\alpha(t)$ as (17). The gain of the linear block is chosen as $c = 10$.

Fig. 5a shows the Power Spectral Density (PSD) of the signal at the NIS input. Fig. 5b and 5d shows the signal PSD at the NIS output, for the constant and the time varying $\alpha(t)$, respectively. The x-axis shows the frequency in GHz with reference to f_d. As shown in Fig. 5a, SIR at the NIS input is -60 dB. Bandwidth of the GSM signal is 100 times smaller than bandwidth of WLAN signal. Hence the PSD of the GSM signal will be 80 dB larger at the NIS input. The input channel noise is filtered by the BPF1 and is centered about f_d.

As shown in Fig. 5b, at the NIS output the interference is attenuated and its power is much smaller than the desired signal power. The desired signal power is increased by 14 dB which is the result of the NIS gain of $20\log_{10}(\frac{c}{2}) = 14$ dB for the desired signal. Also an intermodulation with a power equal to the desired signal is seen at the NIS output as predicted by the analysis in section II-B.

In Fig. 5c we see the un-coded SER for the RX with the NIS vs. SIR$_x = \frac{P_d}{P_i}$, which is slightly higher than 10^{-3} (SER of an exactly linear RX). This small degradation, which increases when SIR$_x$ increases, originates from the nonlinear distortion and the disturbance term in (13). Both of these degradations increase when P_d becomes close to P_i, as predicted by (9) and (13), respectively. For smaller SIR$_x$, SER approaches 10^{-3}. For larger SIR$_x$, the receiver can handle the interferer without using the NIS. Hence the receiver can operate in the complete range of SIR$_x$ with a negligible degradation to SER performance while we have achieved interference suppression which leads to substantial reduction of the RX power consumption.

As shown in Fig. 5d for the time varying $\alpha(t)$, the interferer power at the NIS output is about the same as that of the desired signal. This verifies that with the chosen value for μ_0 the feedback loop is fast enough to track $\alpha(t)$ with a sufficiently small

error. With this amount of suppression, further suppression of the interferer can be done in the subsequent stages of the receiver, without requiring an excessive dynamic range.

V. Conclusion

In multimode transceivers, the interferer induced by the local transmitter can be several orders of magnitude larger than the desired signal, even after partial suppression by analog filters. Hence the receiver requires an excessive linear dynamic range to process the desired signal in the presence of such a large interferer, which leads to an unreasonable power consumption. Several potential interferers in multimode transceivers have Constant Modulus (CM) modulations. An existing solution uses a memoryless Nonlinear circuit, tuned with an open-loop method, to suppress a CM interferer. However the required accuracy for the this method cannot be easily achieved. To overcome this problem, we proposed a closed-loop tuning method which also exploits the available knowledge on the transmitted interferer. We showed that the proposed method can suppress the interferer to a level below that of the desired signal while introducing negligible distortion. The simulations for a practical multimode scenario confirm these results and promise a substantial reduction of transceiver power consumption.

Appendix I. Derivation of the error signal

The switching mixing described in (12) is equivalent to multiplying $y(t)$ by $x_L(t) = \text{sign}(x(t))$. Taking the sign of $x(t)$ is equivalent to passing it through a hard limiter. Using the analysis in [8] for a bandpass limiter when $A_i >> A_d(t)$, $x_L(t)$ is obtained as:

$$\begin{aligned} x_L(t) \simeq \frac{4}{\pi}(\cos(2\pi f_i t + \varphi_i(t)) + \frac{A_d(t)}{2A_i(t)}\cos(2\pi f_d t + \varphi_d(t)) \\ - \frac{A_d(t)}{2A_i(t)}\cos(2\pi(2f_i - f_d)t + 2\varphi_i(t) - \varphi_d(t))) \\ + \text{high frequency components around } 3f_d,\ 3f_i,\ 5f_i,... \end{aligned}$$

The BPF2 if Fig. 3 filters out the high frequency components of $y(t)$ such that only the components around f_d and f_i are remained. Thus it is sufficient to only consider the component of $x_L(t)$ around f_i and f_d. The mixer output $\eta(t)$ is obtained as:

$$\begin{aligned} \eta(t) \simeq x_L(t)y(t) = \frac{2}{\pi}(A_{i,y}(t) + A_{d,y}(t)\frac{A_d(t)}{2A_i(t)} - A_{\text{IM}}(t)\frac{A_d(t)}{2A_i(t)} \\ + \left(A_{d,y}(t) + A_{i,y}(t)\frac{A_d(t)}{2A_i(t)}\right)\cos(2\pi(f_d - f_i)t + \varphi_d(t) - \varphi_i(t)) \\ + \text{Hight frequency components around } 2f_d,\ 2f_i,\ 2f_i - 2f_d,... \end{aligned}$$

Because of the low pass nature of the feedback loop we can neglect the high frequency components of $\eta(t)$:

$$\begin{aligned} \eta(t) \simeq x_L(t)y(t) = \frac{2}{\pi}(A_{i,y}(t) + A_{d,y}(t)\frac{A_d(t)}{2A_i(t)} - A_{\text{IM}}(t)\frac{A_d(t)}{2A_i(t)} \\ + A_{d,y}(t)\cos(2\pi(f_d - f_i)t + \varphi_d(t) - \varphi_i(t)). \end{aligned} \quad (18)$$

In (18) we have neglected the components with center frequencies higher than $f_d - f_i$. Also the component at $f_d - f_i$ that has an envelope of $A_{i,y}(t)\frac{A_d(t)}{2A_i(t)}$ which is much smaller than $A_{d,y}(t)$ is also neglected. Using (3), (2), (5), and considering that during the GSM transmission ($|i(t-\tau) = 1|$), we obtain:

$$A_{d,y}(t) \simeq (\frac{\hat{k}}{2k} - 1)cA_d(t), \quad A_{\text{IM}}(t) \simeq -\frac{\hat{k}}{2k}cA_d(t) \quad (19)$$

Using (10), (18) and (19), (13) is obtained.

Acknowledgment

This work was funded by the Netherlands technology foundation (STW) within Digitally Enhanced And Controlled Front-Ends (DECAFE) project. The authors would like to thank Henk ten Pierick and Hendrik van der Ploeg of Catena for their fruitful discussions.

References

[1] L. Maurer, "Adaptive digital front-end enhanced CMOS-based RF transceivers a brief overview," *Integrated Nonlinear Microwave and Millimetre-Wave Circuits, 2008. INMMIC 2008. Workshop on*, pp. 111 –114, Nov. 2008.

[2] J. Zhu, A. Waltho, X. Yang, and X. Guo, "Multi-radio coexistence: challenges and opportunities," *Proceedings of 16th International Conference on Computer Communications and Networks, 2007. ICCCN 2007.*, pp. 358 –364, Aug. 2007.

[3] B. Razavi, *RF Microelectronics*. Upper Saddle River, NJ, USA: Prentice-Hall, Inc., 1998.

[4] W. Sheng, A. Emira, and E. Sanchez-Sinencio, "CMOS RF receiver system design: a systematic approach," *IEEE Transactions on Circuits and Systems I: Regular Papers*, vol. 53, no. 5, pp. 1023 – 1034, May. 2006.

[5] A. Dejonghe, B. Bougard, S. Pollin, J. Craninckx, A. Bourdoux, L. Ven der Perre, and F. Catthoor, "Green reconfigurable radio systems," *IEEE Signal Processing Magazine*, vol. 24, no. 3, pp. 90 –101, May. 2007.

[6] N. Blachman, "Optimum memoryless bandpass nonlinearities," *Communications, Speech and Vision, IEE Proceedings I*, vol. 140, no. 6, pp. 436 –444, Dec. 1993.

[7] P. Baier and K.-J. Friederichs, "A nonlinear device to suppress strong interfering signals with arbitrary angle modulation in spread-spectrum receivers," *IEEE Transactions on Communications*, vol. 33, no. 3, pp. 300–302, Mar. 1985.

[8] C. Cahn, "A note on signal-to-noise ratio in band-pass limiters," *IRE Transactions on Information Theory*, vol. 7, no. 1, pp. 39 –43, Jan. 1961.

[9] A. Gelb and V. V. W. E., *Multiple-Input Describing Functions And Nonlinear System Design*. McGraw-Hill, 1968.

[10] S. Merchan, A. Armada, and J. Garcia, "Ofdm performance in amplifier nonlinearity," *IEEE Transactions on Broadcasting*, vol. 44, no. 1, pp. 106 –114, mar 1998.

[11] J. G. Proakis, *Digital communications*. McGraw-Hill, New York, 1983.